


**Emergence of cooperation through chain-reaction death**Jiwon Bahk <sup>1</sup> and Hyeong-Chai Jeong <sup>1,2</sup><sup>1</sup>*Department of Physics and Astronomy, Sejong University, Seoul 05006, Korea*<sup>2</sup>*School of Physics, Korea Institute for Advanced Study, Seoul 02455, Korea* (Received 1 June 2020; revised 3 August 2021; accepted 25 January 2022; published 11 February 2022)

We generalize the Bak-Sneppen model of coevolution to a game model for evolutionary dynamics which provides a natural way for the emergence of cooperation. Interaction between members is mimicked by a prisoner's dilemma game with a memoryless stochastic strategy. The fitness of each member is determined by the payoffs  $\pi$  of the games with its neighbors. We investigate the evolutionary dynamics using a mean-field calculation and Monte Carlo method with two types of death processes, fitness-dependent death and chain-reaction death. In the former, the death probability is proportional to  $e^{-\beta\pi}$  where  $\beta$  is the "selection intensity." The neighbors of the death site also die with a probability  $R$  through the chain-reaction process invoked by the abrupt change of the interaction environment. When a cooperator interacts with defectors, the cooperator is likely to die due to its low payoff, but the neighboring defectors also tend to disappear through the chain-reaction death, giving rise to an assortment of cooperators. Owing to this assortment, cooperation can emerge for a wider range of  $R$  values than the mean-field theory predicts. We present the detailed evolutionary dynamics of our model and the conditions for the emergence of cooperation.

DOI: [10.1103/PhysRevE.105.024116](https://doi.org/10.1103/PhysRevE.105.024116)**I. INTRODUCTION**

Why do people cooperate even when they can apparently get more by defecting? This "cooperation puzzle" is ubiquitous. On the gene level, a selfish gene survives by copying itself more than its competitors do. At the individual level, the fitter has more offspring. In the coarse-grained level of "quasispecies," the fitter survives longer. Hence, on any level, it seems that we can thrive by choosing the strategies which increase our own fitness. Since the cooperation accompanies cost in general, our fitness is expected to decrease when we cooperate. However, we see cooperation everywhere. Why is this so?

There have been extensive studies and explanations for this cooperation puzzle. They can be categorized (arguably) into five rules: direct reciprocity, indirect reciprocity, kin selection, network reciprocity, and group selection [1–5]. The cooperative phenomena in nature would probably emerge due to the combined effects of these five mechanisms [6–8] although the degree of contribution from each mechanism varies from case to case.

Most of the known mechanisms for the evolution of altruism have a common process, an assortment of individuals carrying the cooperative phenotypes [9,10]. Here we consider the rather common phenomena of a chain reaction [11] and argue that they might be highly effective ways to develop cooperation through such an assortment for the spatial reciprocity [6,7,12–15].

Most biological systems, from individuals to huge ecological systems to human societies, are complex in their compositions and interactions. Therefore, a failure of one part usually results in malfunctions on the interconnected neighbors. For example, extinction of a species may result in another extinction of a species that had a strong interaction

with the former. We can find chain-reaction phenomena in economic systems also. A bankruptcy of a firm may induce another bankruptcy. This "chain-reaction bankruptcy" may result in an economic catastrophe. Here we argue that the catastrophe can boost cooperation and may turn out to be good for the system in the long run although the individuals who are involved in this catastrophe are in pain.

The structure and interaction between members in biological and social systems are complex in general. Yet the essence of the competition for survival in many cases can be often reduced to a social dilemma game in which self-interest favors defection while the best for the system is cooperation. The prisoner's dilemma (PD) game is a standard example that represents interactions in this kind of social dilemma. In the PD game, the payoff of mutual cooperation is better than that of mutual defection, but one gets more payoff when it defects no matter what the opponent does. If all players are rational, i.e., if they behave to maximize their own payoffs, they will arrive at the Nash equilibrium of mutual defection.

It is still under debate whether the rationality assumption of human behaviors is valid. However, rationality develops naturally over generations in the game theory approach of biological evolution where the fitness of a player is given as an increasing function of its payoff [16]. Usually the fitness of an individual is interpreted as its fecundity, the number of its expected offspring. Hence, a population is to evolve on the one consisting of rational players.

In this work we study the evolution of memoryless stochastic strategies of PD games on structured populations. We mainly consider the cycle, which is one of the simplest structures for the sake of mathematical analysis. The results on a scale-free network structure are given in Appendix D. The fitness  $f$  of each member is given by  $f = e^{\beta\pi}$  where  $\pi$  is the total payoffs of PD games with its nearest neighbors.

Here “inverse temperature” or “selection intensity”  $\beta$  represents how strongly the fitness of a member depends on the payoffs of the gamelike interactions with its neighbors. Our model is different from the conventional game dynamics in both death and birth processes. We have two types of death processes: fitness-dependent death (FDD) and chain-reaction death (CRD). In the former, the death rate of a member with fitness  $f = e^{\beta\pi}$  is proportional to  $1/f = e^{-\beta\pi}$ . If an FDD happens, the immediate neighbors of the FDD site may also die with a probability  $R$  through the chain-reaction process. We think that the CRD process may have an element that is hard to be counted via payoff adjustments [17]. When a member dies by either process, it is replaced by a new member, which has a random strategy (rather than the offspring of the neighbors), so that the fitness affects population dynamics only through the death process as in the Bak-Sneppen model [18]. In this sense, a member of the population in our model may represent a quasispecies rather than an individual for a biological system [11,18]. On the other hand, when it applies to an economic system, replacement by a new member can be interpreted as a foundation of a new firm rather than an expansion of a nearby firm. In this paper, CRD is applied to the nearest neighbors of the FDD site only. We may consider a model with iterative CRD. However, we expect its result would not be qualitatively different from the one presented here for the sufficiently large population because the process would end at a finite number of steps unless the bare CRD probability is one.

The CRD is a crucial element for the evolution of cooperation in our model. The fitness in our model is interpreted as longevity (instead of fecundity), and selection acts on death through the FDD. If a player switches its action from cooperation to defection, its death probability in the FDD process decreases while the FDD probabilities of its game partners increase regardless of the strategies of the neighbors. In other words, the competition occurs directly between game partners as in the conventional Birth-Death process [19], and network reciprocity cannot be invoked in the FDD process alone [10,20]. However, in the CRD process, defectors have fewer chances to survive. The neighbors of defectors have lower payoffs on average, i.e., a high chance to disappear by FDD. In other words, defectors are more likely to be located at the neighbors of FDD sites and hence likely to disappear by CRD. In our model, the FDD and CRD processes suppress cooperators and defectors, respectively. Hence, depending on the value of chain-reaction probability  $R$ , population can be either cooperative or defective. Using the mean-field (MF) approximation, we first investigate the MF boundary values,  $R_b^{\text{MF}}$  between the cooperative and the defective phases. We then study the evolutionary dynamics for strongly assortative populations which occurs when  $\beta$  is large. For strong selection, a cooperator is likely to die by FDD when its neighbors are defectors. Subsequently, the exploiter, who makes the cooperator die, is also prone to die through CRD. Therefore, heterogeneous domains in the population disappear first and then patches of homogeneous communities with similar cooperating probabilities evolve. Once these strong assortments are established, group selection arguments can boost the evolution of cooperation. Cooperating communities survive longer than defecting communities due to their high payoffs. For strong selection, we will see that populations become cooperative in a wide range  $R$  values

including the regions where MF theory predicts the defective population.

In the following section, we introduce and define our model precisely. Then we use the MF theory and Monte Carlo (MC) simulation to analyze dynamics and the steady-state properties of our model. In Sec. III we explain these methods and provide the results. A summary and concluding remarks are presented in the final section.

## II. MODEL

We consider a PD game as an interaction between two competitive members in a population. Each player has two possible actions in a single PD game: cooperation (C) or defection (D). The payoff of a player depends on the opponent’s action, as well as his own action. We consider a simplified PD game, called a “donation game,” in which the payoffs are calculated by the cost  $c$  and the benefit  $b$  of a cooperative action. If one player defects while the other cooperates, the defector receives benefit without any cost, whereas the cooperator pays cost and its payoff becomes  $-c$ . For mutual cooperation both get a benefit but pay a cost and their payoffs become  $b - c$ , while the payoffs for mutual defection are 0. Without loss of generality, we set  $b = 1$ . The payoff matrix then becomes

$$\begin{array}{cc} & \begin{array}{cc} C & D \end{array} \\ \begin{array}{c} C \\ D \end{array} & \begin{pmatrix} 1-c & -c \\ 1 & 0 \end{pmatrix}. \end{array}$$

Here  $0 < c < 1$ . When the (equal) gain from switching (from C to D)  $c$  is positive, defection is the individual’s optimal choice, while the social optimum is cooperation as long as the cost is less than the benefit ( $c < 1$ ).

We consider a simple population structure, a cycle of  $N$  sites with game interaction between the nearest neighbors only [8,21,22]. Here a cycle means a finite one-dimensional (1D) lattice with periodic boundary conditions. We assume that each member has a history-independent stochastic strategy, and the phenotype of member  $i$ , the inhabitant at site  $i$ , is represented by its cooperation probability  $q_i$ . The deterministic strategies, “pure C” and “pure D,” correspond to  $q_i = 1$  and  $q_i = 0$ , respectively. The fitness  $f_i$  of member  $i$  is determined by the (expected) total payoffs  $\pi_i$  from the games with its neighbors. On the cycle population,  $\pi_i$  is given by

$$\pi_i = q_{i-1} + q_{i+1} - 2cq_i, \quad (1)$$

where  $i \pm 1$  should be read as  $i \pm 1$  modulo  $N$ . The sum of the first two terms  $q_{i-1} + q_{i+1}$  of Eq. (1) is the expected benefit from the cooperation of the neighbors. The last term  $2cq_i$  is the expected cost of cooperation of member  $i$ . Note that the payoffs of all members in the population at time  $t$  are specified by the population profile of cooperation probabilities  $\{q_i(t) | i \in \{1, \dots, N\}\}$ .

The members in the population die with the two types of death processes, FDD and CRD. In the former, the death rate of member  $i$  is proportional to  $1/f_i = e^{-\beta\pi_i}$  where  $\beta$  is the selection intensity. In the limit of  $\beta$  goes to zero, members die randomly regardless of their fitness while only the least fit (minimum payoff) member dies for infinite  $\beta$ . When FDD occurs at a site, its neighbors may also die by CRD, which occurs with a probability  $R$ . Neighbors of the death site are

expected to be harmed due to abrupt changes in the interaction environment. Once a member dies by either process, its site is occupied by a new member with a random cooperation probability [11,18] which is chosen from the uniform distribution in the interval [0 1].

### III. METHODS AND RESULTS

We study the evolution of the population strategy with MF theory and MC simulations on a cycle of  $N$  sites. The initial state of the population is given as a random configuration, i.e.,  $q_i \in [0, 1]$  with the uniform distribution for  $i = 1, \dots, N$ . At each time step, we calculate the payoffs of all members in the population and choose one site for FDD with a probability  $p_i^d = \frac{1}{Z} e^{-\beta \pi_i}$  where the superscript  $d$  stands for ‘‘death.’’ Here  $\pi_i$  is the payoff of member  $i$  given by Eq. (1), and  $Z = \sum_i e^{-\beta \pi_i}$  is the normalization factor. The cooperation probability for the chosen site is updated with a new random number. The cooperation probabilities of the two neighbors of the FDD site are updated with the probability  $R$  each. We then measure the mean cooperation  $Q = \langle \frac{1}{N} \sum_{i=1}^N q_i \rangle$  as a function of time, where  $\langle x \rangle$  means ‘‘ensemble average’’ of  $x$ . The mean cooperation converges to a steady-state value  $Q_s = Q_s(\beta, c, R)$  at sufficiently late time for a given set of parameters,  $\beta$ ,  $c$ , and  $R$ . The cooperation region in the  $R$ - $c$  parameter space is then obtained using the condition  $Q_s > 1/2$ . We find that the phase diagrams (of the cooperative and defective phases in the  $R$ - $c$  parameter space) are considerably different depending on selection intensity. In the weak selection limit of  $\beta \rightarrow 0$ ,  $Q_s$  is larger than  $1/2$  when  $R > c$ . On the other hand, cooperation emerges for a wide range of  $R$  (unless  $c$  is close to 1) for strong selection.

We first consider the MF dynamics. In the MF approximation, all neighbors of a given individual are assumed to show the average behaviors of the population. The MF results are expected to be valid in the weak selection limit where the survival probability of a member is almost independent of its strategy, and hence no correlation between neighboring members is developed. The MF study for strong selections also can be useful. By comparing the MC dynamics with MF approximation, we may have a better understanding of how strong cooperation evolves on the population with strong selection. For these reasons, we present the MF calculation before presenting the MC results.

#### A. Mean-field approximation

In the MF approximation, all neighbors of a given member have the same average cooperation probability  $Q^{\text{MF}}$ . For a given  $q_i$ , the payoffs  $\pi_i$  and  $\pi_{i\pm 1}$  become

$$\pi_i = 2Q^{\text{MF}} - 2cq_i, \quad \pi_{i\pm 1} = q_i + Q^{\text{MF}} - 2cQ^{\text{MF}}, \quad (2)$$

where we have replaced  $q_{i\pm 1}$  and  $q_{i\pm 2}$  by  $Q^{\text{MF}}$  in Eq. (1). The death rates  $r_i^{\text{FDD}}$  and  $r_i^{\text{CRD}}$  of member  $i$  for the FDD and CRD processes satisfy

$$\begin{aligned} r_i^{\text{FDD}} &\propto e^{-\beta \pi_i} \propto e^{2\beta c q_i}, \\ r_i^{\text{CRD}} &\propto R(e^{-\beta \pi_{i+1}} + e^{-\beta \pi_{i-1}}) \propto 2R e^{-\beta q_i}. \end{aligned} \quad (3)$$

When member  $i$  dies,  $q_i$  is replaced by a new random number chosen from the uniform distribution between 0 and 1. Hence,

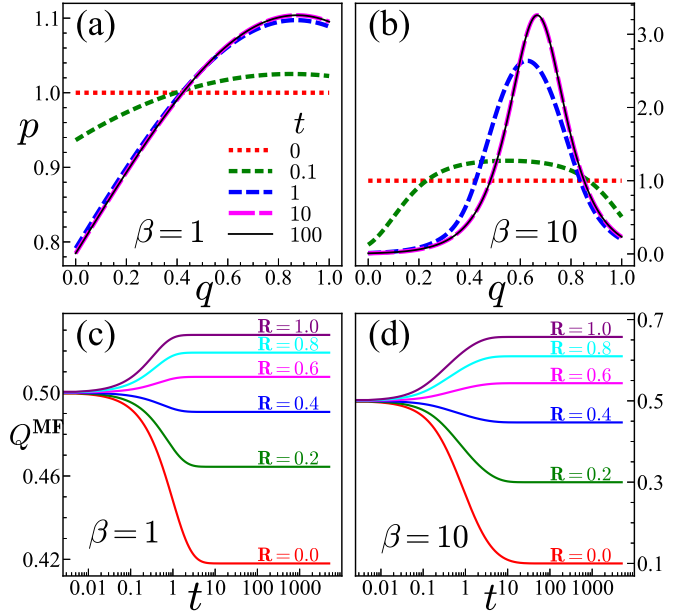


FIG. 1. Evolution of the PDF  $p(q, t)$  and the mean cooperation  $Q^{\text{MF}}(t)$  in the MF theory. For two different selection intensities, (a)  $\beta = 1$  and (b)  $\beta = 10$ ,  $p(q, t)$  for  $R = 1$  at five different times,  $t = 0, 0.1, 1, 10$ , and  $100$ , are shown. In (c) and (d),  $Q^{\text{MF}}$  is plotted against time  $t$  in a semilog scale for six different values of  $R = 0.0, 0.2, 0.4, 0.6, 0.8$ , and  $1.0$  for  $\beta = 1$  and  $\beta = 10$ , respectively. The y-axis labels and legends in (a) and (c) are applied to (b) and (d), respectively. For all cases, we use  $c = 0.5$ .

the probability density function (PDF)  $p(q, t)$  in the MF theory evolves [23] as

$$\begin{aligned} p(q, t + \Delta t) = p(q, t) + \frac{1 + 2R}{N} \frac{1}{N} \frac{e^{2\beta c q} p(q, t)}{\int_0^1 e^{2\beta c q} p(q, t) dq} \\ - \frac{2R}{N} \frac{e^{-\beta q} p(q, t)}{\int_0^1 e^{-\beta q} p(q, t) dq}, \end{aligned} \quad (4)$$

from the initial distribution  $p(q, 0) = 1$  for  $0 \leq q \leq 1$ . Here  $N$  is the population size and  $\Delta t = 1/N$  since we take  $N$  such updates as unit time. Once we get a PDF  $p(q, t)$ , we can calculate the mean cooperation  $Q^{\text{MF}}(t)$  in the MF approximation by

$$Q^{\text{MF}}(t) = \int_0^1 q p(q, t) dq. \quad (5)$$

Figure 1 shows the evolution of the PDF  $p(q, t)$  and the mean cooperation  $Q^{\text{MF}}(t)$  for  $c = 0.5$  in the MF theory. In Figs. 1(a) and 1(b),  $p(q, t)$  for  $R = 1$  are shown at five different times,  $t = 0, 0.1, 1, 10$ , and  $10^2$  with  $\beta = 1$  and  $\beta = 10$ , respectively. Initially, the distributions are uniform as indicated by the red dotted lines. The PDF  $p(q, t)$  for  $t > 0$  is obtained by Eq. (4) (with  $N = 200$ ). As shown in (a),  $p(q, t)$  for  $\beta = 1$  initially increases for  $q > q_* \approx 0.422$  and decreases for  $q < q_*$  with time. The population then reaches a steady state around  $t = 10$ . The PDF at  $t = 10^2$  is almost identical to that at  $t = 10$ . Hence, we believe that the black solid line of  $t = 10^2$  represents the steady-state PDF. Similarly, we calculate the PDF for  $\beta = 10$  and show this in (b). In this strong

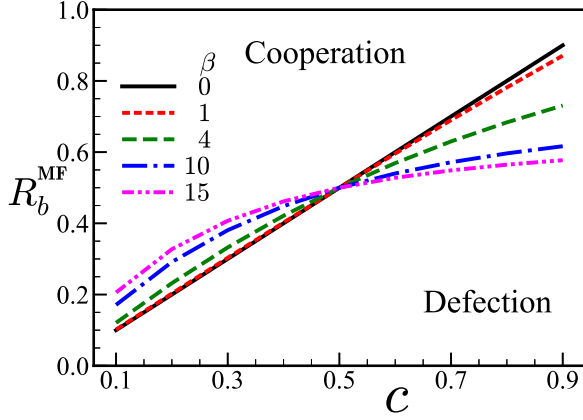


FIG. 2. The MF boundaries between cooperative and defective phases in the  $R$ - $c$  parameter space are presented for  $\beta = 0, 1, 4, 10$ , and  $15$ .

selection case, PDF for large  $q$  near 1 is also decreasing such as that for small  $q$  initially. The decreasing range for a small  $q$  region increases with time for a while and then reaches the steady-state PDF. As one can see from the black solid line in (b), the steady-state PDF for  $\beta = 10$  is narrow compared to the  $\beta = 1$  case and has a single peak around  $q = 0.667$ .

The mean cooperation  $Q^{\text{MF}}(t)$  is then calculated using Eq. (5). Figures 1(c) and 1(d) show  $Q^{\text{MF}}(t)$  for  $\beta = 1$  and  $\beta = 10$ , respectively. Initially, the mean cooperation is  $Q^{\text{MF}}(0) = 0.5$  because the population starts from the uniform PDF. When  $R = c = 1/2$ ,  $Q^{\text{MF}}(t)$  remains as  $0.5$  always for all  $\beta$  as shown in Appendix A. We expect  $Q^{\text{MF}}(t)$  to increase (decrease) with time for  $R > 1/2$  [ $R < 1/2$ ] because the larger  $R$  implies the more CRD processes which diminish the exploiters and promote cooperators. We can confirm such behaviors for both selection intensities as shown in Figs. 1(c) and 1(d). As  $R$  deviates from  $1/2$ , so does the mean cooperation value  $Q_s^{\text{MF}}$  in the steady states.

We now investigate the cooperative region in the  $R$ - $c$  parameter space by finding the condition for  $Q_s^{\text{MF}}$  to be larger than  $1/2$ . For a given selection intensity  $\beta$ , we vary the cost  $c$  from 0 to 1 with  $\Delta c = 0.1$  steps and calculate  $Q_s^{\text{MF}}$  for a series of  $R$  values to find  $R_b^{\text{MF}}(\beta, c)$  such that  $Q_s^{\text{MF}}(\beta, c, R_b^{\text{MF}}) = 1/2$ . This MF boundaries  $R_b^{\text{MF}}$  between the cooperative and defective regions in the  $R$ - $c$  parameter space are mostly obtained numerically except for the weak selection limit of  $\beta \rightarrow 0$ . In this limit, the boundary between two regions is given by  $R_b^{\text{MF}} = c$  as shown in Appendix B.

Figure 2 shows the  $R_b^{\text{MF}}$  lines for four different values of selection intensities,  $\beta = 1, 4, 10$ , and  $15$  together with the analytic solution for  $\beta \rightarrow 0$ . The black line of  $R_b^{\text{MF}} = c$  is the boundary for the weak selection limit of  $\beta \rightarrow 0$ . The red dotted line of  $\beta = 1$  is almost identical to  $R_b^{\text{MF}} = c$  except for the large  $c$  region. For strong selection,  $R_b^{\text{MF}}$  behaves differently depending on the cost values. As  $\beta$  increases,  $R_b^{\text{MF}}$  also increases for  $c < 1/2$ , but it decreases for  $c > 1/2$ . These behaviors are quite opposite to what is observed in the MC simulations. As we will see below, the correlations between FDD sites, which are ignored in the MF theory, play an important role for strong selection cases and make the population evolve differently from MF theory.

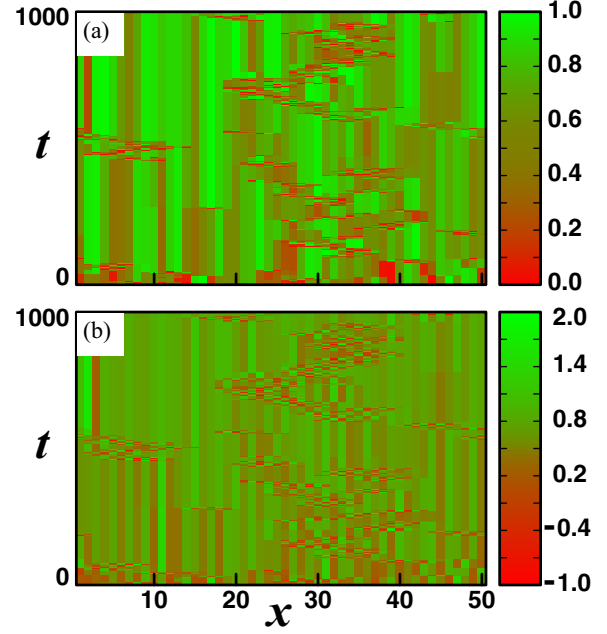


FIG. 3. Evolution of (a) cooperation probability  $q_i$  and (b) payoff  $\pi_i$  from  $t = 0$  to  $t = 1000$  for  $i \in \{0, \dots, 50\}$ . Their values are represented by colors indicated by the right panels. Here  $c = 0.5$ ,  $R = 1$ ,  $\beta = 100$ , and  $N = 50$ .

## B. Monte Carlo simulation

In this section, our Monte Carlo (MC) methods and results are presented. We perform a series of MC simulations and measure the mean cooperations  $Q(t)$  for various selection intensities  $\beta$ , cost values  $c$ , and chain-reaction probabilities  $R$ . The detailed MC procedure is as follows. (1) Construct a cycle population of size  $N$ . (2) Choose a random number from the uniform distribution in the interval  $[0, 1]$  and assign it as  $q_i$  for  $i = 1, \dots, N$ . (3) Calculate the payoff  $\pi_i$  of member  $i$  using Eq. (1) for  $i = 1, \dots, N$ . (4) Choose an FDD site  $i$  with the probability

$$p_i^d = \frac{1}{\sum_j e^{-\beta\pi_j}} e^{-\beta\pi_i}, \quad (6)$$

and assign a new random number  $q_i$ . (5) Assign new random numbers  $q_{i-1}$  and  $q_{i+1}$  with the probabilities  $R$  for each. (6) The  $N$  repeats of (4) and (5) are defined as a MC step (MCS) which is taken as a unit time.

Figure 3 shows the configurations of cooperation probabilities  $q_i$  and payoff  $\pi_i$  for an initial 1000 MCS of a population of size  $N = 50$ . Parameters used in this example are  $c = 0.5$ ,  $R = 1$ , and  $\beta = 100$ . The cooperation probability  $q_i$  and the payoff  $\pi_i$  at the site  $i$  are represented by colors, as shown in the right panels. Initially ( $t = 0$ ), all  $q_i$  values are selected from a uniform distribution from 0 to 1. A sudden change of the color in a vertical column implies the death and replacement of the member at the site. We first note that overall structure evolves to a cooperative (green) population. Green sites are more common for a later time. Also, we find that green columns tend to aggregate as time goes by. In other words, the population develops assortments of cooperators. The average lifetime of the defective [red (dark gray)] sites

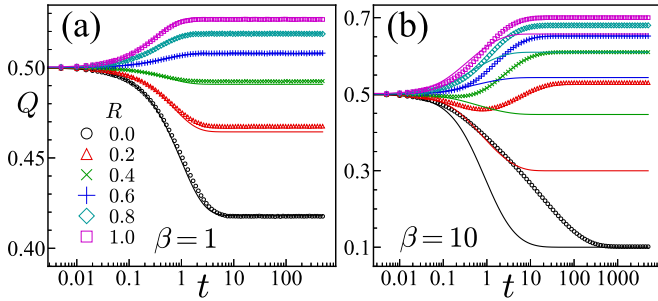


FIG. 4. The mean cooperation  $Q(t)$  measured in MC (symbols) are compared with the MF values (lines). MC data are obtained using the population of size  $N = 200$  with  $c = 0.5$  at six different values of  $R = 0, 0.2, 0.4, 0.6, 0.8,$  and  $1$  for (a)  $\beta = 1$  and (b)  $\beta = 10$ . For  $\beta = 1$ , MC results are consistent with MF calculation, but deviation from the MF is manifested for  $\beta = 10$ .

is much smaller than that of cooperative [green (light gray)] sites. The death and replacement activities are localized near the red sites. These features explain qualitatively how cooperation evolves in our model at large  $\beta$  values. A cooperator in the middle of defectors has a small fitness and tends to die out by FDD. Newcomers at the site cannot survive unless they are defectors. Hence, the defector abundant regions become a homogeneous defective (D) community. On the other hand, a cooperator in the middle of cooperators lives long due to its high payoff and forms a cooperative (C) community easily. Therefore, the population develops strong assortments in a relatively short time. In the long run, the population becomes cooperative since the average lifetime of the members in a D community is shorter than that in a C community.

For a quantitative analysis, we now repeat  $M$  independent simulations and measure the average of the mean cooperation  $Q(t)$  at time  $t$  defined by

$$Q(t) = \left\langle \frac{1}{N} \sum_{i=1}^N q_i(t) \right\rangle = \frac{1}{MN} \sum_{m=1}^M \sum_{i=1}^N q_i^{(m)}(t), \quad (7)$$

where  $q_i^{(m)}(t)$  is the cooperation probability of member  $i$  at time  $t$  in the  $m$ th simulation. Figure 4 shows the mean cooperation  $Q(t)$  with  $c = 0.5$  for two different values of selection intensities (a)  $\beta = 1$  and (b)  $\beta = 10$  together with the MF data from Figs. 1(c) and 1(d). In both cases, the mean cooperation values are measured for six different values of the chain-reaction probabilities,  $R = 0.0, 0.2, 0.4, 0.6, 0.8,$  and  $1$ . The mean cooperation values are plotted in a semilog scale to show the initial dynamics in detail, as well as the long-time evolutions.

The strategies of the initial population are given randomly. Hence,  $Q(t)$  is expected to follow the MF dynamics at the beginning. In fact, we see that the mean cooperation  $Q(t)$  for  $\beta = 10$  as well as for  $\beta = 1$  follows the MF values in the early time ( $t < t_i \approx 0.1$ ). At a sufficiently later time,  $Q(t)$  converges to its steady-state value  $Q_s$  although the time to reach  $Q_s$  depends on  $\beta$  and  $R$  values. For  $\beta = 1$ , MC results are consistent with the MF calculation quite well for all time. Even in the steady states, mean cooperations  $Q_s$  are not much different from the MF values  $Q_s^{\text{MF}}$ . However, for a strong selection, deviations from the MF values are manifested for

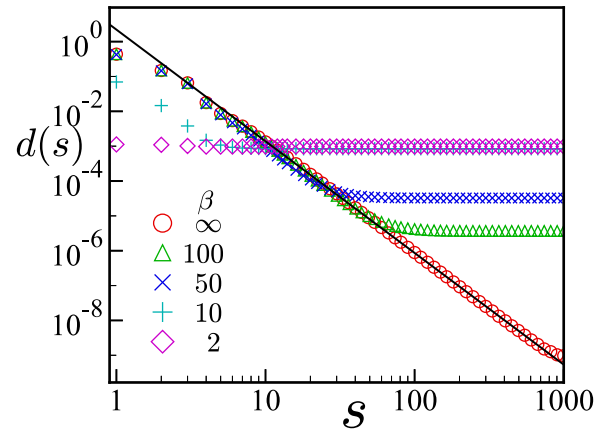


FIG. 5. Distribution  $d(s)$  of the distances  $s$  between successive FDD sites for five different selection intensities  $\beta = 2, 10, 50, 100,$  and  $\infty$ . For all cases, populations of  $N = 2048$  are used with the parameters  $c = 0.5$  and  $R = 1$ .

$t > t_i$ . After following the initial MF-like dynamics,  $Q(t)$  for  $\beta = 10$  becomes larger than MF values in most cases. The only exception is the steady-state value  $Q_s$  of  $R = 0$ . It is almost the same as the MF value. These results are consistent qualitatively with our previous observation on the configuration evolution in Fig. 3. Before the correlation between FDD sites develops, the population evolves with MF dynamics, but once the FDD correlation is established, dynamics deviates from MF quite drastically. First, it takes longer to get into the steady state since not all FDD sites are independent. Second, FDD correlation induces an assortment of cooperators for  $R > 0$  so that it boosts the cooperation. For  $\beta = 10$  shown in Fig. 4(b), the mean cooperation becomes larger than  $1/2$  at a later time even for  $R = 0.2$  (red triangles) while  $R_b^{\text{MF}}$  is only  $0.3$ . For  $R = 0$ , FDD correlation is developed, but it does not promote cooperation due to a lack of the CRD process. Hence, the time to reach the steady state is longer than the MF case's, but  $Q_s$  is almost identical to  $Q_s^{\text{MF}}$ .

We now measure the distance distributions between successive FDD sites in the steady states to find correlation lengths [11,18]. Figure 5 shows the distribution  $d(s)$  of the distances  $s$  between successive FDD sites measured for  $c = 0.5$  and  $R = 1$  at five different values of selection intensities,  $\beta = 2, 10, 50, 100,$  and  $\infty$  using the population of  $N = 2048$ . When the distributions  $d(s)$  are plotted against  $s$  in a log-log scale, they lie on a single line indicating power-law distributions  $d(x) \sim x^{-\alpha}$  up to the correlation lengths  $\xi$  which depend on the selection intensities. From the figure, we estimate the correlation lengths  $\xi = 3.88, 4.73, 28.4, 64.5,$  and  $\infty$  for  $\beta = 2, 10, 50, 100,$  and  $\infty$ , respectively. The power-law exponent  $\alpha$  is around  $\alpha = 3.2 \pm 0.1$ . This exponent is similar to the known exponent  $\alpha = 3.15 \pm 0.05$  of the 1D BS model [18]. The power law for  $\beta = \infty$  indicates that the evolution occurs in a dynamical criticality [18,24].

As in the MF calculation, we use the criterion of  $Q_s > 1/2$  to identify the cooperative region in the  $R$ - $c$  parameter space. We choose five different values of selection intensities,  $\beta = 1, 4, 10, 100,$  and  $\infty$ , and perform a series of Monte Carlo simulations to find  $R_b$  such that  $Q_s(\beta, c, R_b) = 1/2$  for nine

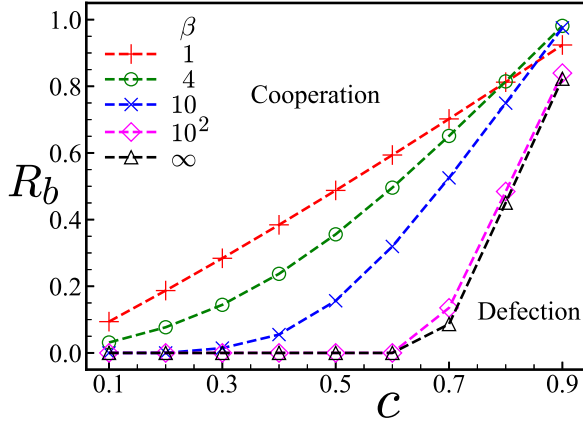


FIG. 6. The boundaries between cooperative and defective phases in the  $R$ - $c$  parameter space are presented for  $\beta = 1$  (pluses), 4 (circles), 10 (crosses),  $10^2$  (diamonds), and  $\infty$  (triangles).  $R_b$  values are obtained at  $c = 0.1, 0.2, \dots, 0.9$  for each  $\beta$ .  $N = 200$  for all cases.

different cooperation costs,  $c = 0.1, 0.2, \dots, 0.9$  for each selection intensity. Figure 6 shows the boundaries between the cooperative region ( $Q_s > 1/2$ ) and the defective region ( $Q_s < 1/2$ ) in the  $R$ - $c$  parameter space. They are obtained by MC simulations on a population of size  $N = 200$ . The plus, circle, diamond, and triangle symbols are used to denote the  $R_b$  values for  $\beta = 1, 4, 10, 100$ , and  $\infty$ , respectively.

We would like to emphasize that  $R_b$  values in Fig. 6 are obtained from the simulations on the population of finite size ( $N = 200$ ). We believe that the boundaries between the cooperative and defective regions for  $N = \infty$  would not be much different from those in Fig. 6 for  $\beta = 1, 4, 10$ , and  $100$  cases. For finite selection intensities, the correlation lengths are smaller than the population size used here (see Fig. 5.). However, the correlation length for the  $\beta = \infty$  case seems to diverge. Hence,  $N = 200$  is not big enough to estimate  $R_b$  for  $\beta = \infty$ . As one can see in Fig. 6, for the strong selection limit,  $R_b$  (from simulation on the  $N = 200$  population) is practically zero for  $c < c_c \approx 0.6$  but finite for  $c > c_c$ . We believe that  $R_b$  for the infinite population is also zero for  $c < c_c$ . For large costs ( $c > c_c$ ), we cannot predict with certainty whether  $R_b$  is finite or not, but we speculate that it may remain finite. In Appendix C, the  $R_b$  values for the infinite population are investigated for  $c = 0.8$  and  $0.9$  using a series of populations with increasing sizes. They are well fitted by  $R_b(N) = R_b^\infty - AN^{-\gamma}$  with  $R_b^\infty = 0.38$  and  $0.78$  for  $c = 0.8$  and  $0.9$ , respectively, with  $\gamma = 0.65$  for both cases. We do not know if this trend will continue to the infinite population, but these results make us think that  $R_b^\infty$  remains as finite at least for some large cost values.

Note that  $R_b$  values in Fig. 6 for large cost values for strong selections are larger than  $R_b^{\text{MF}}$  values in Fig. 2. For example, for  $\beta = 10$ ,  $R_b = 0.975$ , while  $R_b^{\text{MF}} = 0.617$  at  $c = 0.9$ . We think this is because the assortment of cooperators is not good enough for the population to be cooperative for a large cost. When  $c$  is large, the assortment does not seem to prevent the invasion of defectors. The CRD process in our model still prevents an invasion of defectors in the middle of a C community, but it can be vulnerable to attack at the boundary. Imagine a

population consisting of two uniform communities, cooperators at  $i \leq N/2$  (with the cooperation probability  $q^C > 1/2$ ) and defectors at  $i > N/2$  (with the cooperation probability  $q^D < 1/2$ ) on a 1D lattice. The payoff  $\pi^{\text{Bc}}$  at the boundary site  $k = N/2$  of the C community is given by

$$\pi^{\text{Bc}} = (q^C + q^D) - (2cq^C) = (1 - 2c)q^C + q^D. \quad (8)$$

On the other hand, the payoff  $\pi^{\text{D}}$  of a defector in the middle of the D community is given by

$$\pi^{\text{D}} = 2(1 - c)q^D. \quad (9)$$

Therefore,  $\pi^{\text{Bc}}$  is smaller than  $\pi^{\text{D}}$  for  $c > 1/2$  and a  $k = N/2$  site is likely to be an FDD site for large  $\beta$ . Let us assume that it has died by an FDD process and a newly assigned  $q_k$  is a midpoint between  $q^C$  and  $q^D$ , i.e.,  $q_{N/2} = (q^C + q^D)/2$ . Then site  $n = N/2 - 1$  becomes the new boundary of C community, and its payoff is given by

$$\begin{aligned} \pi_n &= q^C + (q^C + q^D)/2 - 2cq^C \\ &= \frac{1}{2}[(3 - 4c)q^C + q^D]. \end{aligned} \quad (10)$$

Comparing it with  $\pi^{\text{D}} = 2(1 - c)q^D$ , we see that  $\pi_n$  is smaller than  $\pi^{\text{D}}$  for  $c > 3/4$ . Hence, in this hypothetical population, the C community can be invaded by a defector for  $c > 3/4$ . In real simulations, both C and D communities do not have the uniform cooperation probabilities, but this example may explain why the assorted population can be less cooperative than the MF prediction for large  $c$ . The CRD processes invoke the correlation between FDD sites and help the cooperators and defectors make their own communities, but D communities rather than C communities proliferate when the cost to benefit ratio is close to 1.

#### IV. SUMMARY AND CONCLUDING REMARKS

We have generalized Bak-Sneppen model to an evolutionary game theory and showed that the chain-reaction element of the Bak-Sneppen dynamics could provide a natural way for the evolution of cooperation. In most conventional studies, the success of a strategy was measured by its payoff only. Here, using the concept of chain-reaction bankruptcy, we introduced the CRD process in addition to the FDD process to the evolutionary dynamics. Considering the disadvantage of an abrupt interaction environment change, we think that CRD is a natural phenomenon which can be widely found in many evolutionary systems. It provides one of the simplest ways to suppress the proliferation of defectors. However, to the authors' knowledge, it has not been studied seriously as a mechanism for the evolution of cooperation. We have developed the MF theory and performed a series of MC simulations for strategy evolution when the CRD process coexisted with the FDD process and provided a phase diagram in the  $R$ - $c$  parameter space. For strong selection, we showed that the CRD process introduced strong spatiotemporal correlations between strategies. These correlations invoked the assortment of cooperators and made the population more cooperative than the MF theory predicted for most cases.

In this work, we investigated a rather small strategy space, memoryless stochastic strategies on a simple population structure. However, we believe that our main results, the emergence

of strong cooperation through the assortment of cooperators invoked by the CRD, would be valid for population structure variation as well as the strategy space extension. Preliminary results with the extended strategy space show that the cooperation emerges more easily and rapidly when we included reactive strategies.

Our study may also have natural implication in economical systems because the chain-reaction bankruptcy is a quite feasible scenario. The interaction network is in the real world is complex and far from a simple cycle structure, but we can still define the distance between two firms in terms of minimum number of edges to connect them. It might be worthwhile analyzing bankruptcy data to see if they show any criticality characterized by the power-law distribution in the size of bankruptcy and the correlation between successive bankruptcy. Future research may also investigate the ecological data on the correlation of death tolls.

#### ACKNOWLEDGMENTS

We would like to thank Sunhee Chae and Nahyeon Lee for many useful discussions. This work was supported by a National Research Foundation of Korea (NRF) grant funded by the Korean government (MSIT) (No. NRF-2021R1F1A1063238).

#### APPENDIX A: MEAN COOPERATION IN MF THEORY FOR $c = R = 1/2$

We show that the mean cooperation  $Q$  is  $1/2$  always for  $c = R = 1/2$  in MF theory for all  $\beta$ . For  $c = 1/2$  and  $R = 1/2$ , we see that  $\Delta p \equiv p(q, t + \Delta t) - p(q, t)$  is given by

$$\Delta p(q, t) = \frac{1}{N} [1 - D_F + 2R(1 - D_C)] \quad (\text{A1})$$

$$= \frac{1}{N} [2 - D_F - D_C] \quad (\text{A2})$$

from Eq. (4). Here  $D_F$  and  $D_C$  are the probability densities to die by FDD and CRD processes per unit time, respectively. They are given by

$$D_F(q, t) = \frac{e^{\beta q} p(q, t)}{\int_0^1 e^{\beta q} p(q, t) dq}, \quad (\text{A3})$$

$$D_C(q, t) = \frac{e^{-\beta q} p(q, t)}{\int_0^1 e^{-\beta q} p(q, t) dq}. \quad (\text{A4})$$

If the distribution  $p(q, t)$  has the mirror symmetry of  $p(q, t) = p(1 - q, t)$ , we have

$$D_F(1 - q, t) = \frac{e^{\beta(1-q)} p(1 - q, t)}{\int_0^1 e^{\beta q} p(q, t) dq} \quad (\text{A5})$$

$$= \frac{e^{\beta} e^{-\beta q} p(1 - q, t)}{e^{\beta} \int_0^1 e^{-\beta(1-q)} p(q, t) dq} \quad (\text{A6})$$

$$= \frac{e^{\beta} e^{-\beta q} p(q, t)}{-e^{\beta} \int_1^0 e^{-\beta s} p(1 - s, t) ds} \quad (\text{A7})$$

$$= \frac{e^{\beta} e^{-\beta q} p(q, t)}{e^{\beta} \int_0^1 e^{-\beta s} p(s, t) ds} \quad (\text{A8})$$

$$= D_C(q, t). \quad (\text{A9})$$

By substituting  $q = 1 - q$  in Eq. (A9), we also get  $D_C(1 - q, t) = D_F(q, t)$  and  $\Delta p(1 - q, t) = \Delta p(q, t)$ . This implies that if the distribution  $p(q)$  has the mirror symmetry at  $t$ , so it does at  $t + \Delta t$ . We start from the uniform distribution, which certainly satisfies  $p(1 - q, 0) = p(q, 0)$ . Therefore,  $p(q, t)$  has the mirror symmetry, and the mean cooperation  $Q^{\text{MF}}$  is given by

$$Q^{\text{MF}} = \int_0^1 q p(q) dq \quad (\text{A10})$$

$$= \frac{1}{2} \left[ \int_0^1 q p(q) dq + \int_0^1 (1 - q) p(1 - q) dq \right] \quad (\text{A11})$$

$$= \frac{1}{2} \int_0^1 [q + (1 - q)] p(q) dq \quad (\text{A12})$$

$$= \frac{1}{2} \int_0^1 p(q) dq \quad (\text{A13})$$

$$= \frac{1}{2} \quad (\text{A14})$$

for all  $t$ .

#### APPENDIX B: MF CALCULATION OF $R_b^{\text{MF}}$ FOR $\beta \rightarrow 0$

For the weak selection limit of  $\beta \rightarrow 0$ , we calculate  $p(q, t)$  and  $Q^{\text{MF}}(t)$  in the linear order of  $\beta$  with initial uniform distribution. When the initial distribution is uniform, i.e.,  $p(q, 0) = 1$  for  $0 \leq q \leq 1$ , the distribution change  $\Delta p_0$  between  $t = 0$  and  $t = \Delta t = 1/N$  is given by

$$\Delta p_0 = p(q, \Delta t) - p(q, 0) \quad (\text{B1})$$

$$= \frac{1}{N} \left[ \left( 1 - \frac{e^{2\beta c q}}{\int_0^1 e^{2\beta c q} dq} \right) + 2R \left( 1 - \frac{e^{-\beta q}}{\int_0^1 e^{-\beta q} dq} \right) \right] \quad (\text{B2})$$

$$= \frac{\beta}{N} (c - R)(1 - 2q), \quad (\text{B3})$$

where we used Eq. (4) and ignored the  $O(\beta^2)$  term. Now we calculate  $\Delta p_1$  using Eq. (4) and  $p(q, \Delta t) = 1 + \Delta p_0$  and obtain

$$\Delta p_1 = p(q, 2\Delta t) - p(q, \Delta t) \quad (\text{B4})$$

$$= \frac{\beta}{N} \left( 1 - \frac{1 + 2R}{N} \right) (c - R)(1 - 2q) \quad (\text{B5})$$

and

$$p(q, 2\Delta t) = p(q, \Delta t) \Delta p_1 \quad (\text{B6})$$

$$= 1 + \Delta p_0 + \Delta p_1. \quad (\text{B7})$$

Applying this process iteratively, we get

$$\Delta p_k = p(q, (k + 1)\Delta t) - p(q, k\Delta t) \quad (\text{B8})$$

$$= \frac{\beta}{N} \left( 1 - \frac{1 + 2R}{N} \right)^k (c - R)(1 - 2q) \quad (\text{B9})$$

and

$$p(q, k\Delta t) \quad (\text{B10})$$

$$= 1 + \sum_{j=0}^{k-1} \Delta p_j \quad (\text{B11})$$

$$= 1 + \frac{\beta(c-R)(1-2q)}{N} \sum_{j=0}^{k-1} \left(1 - \frac{1+2R}{N}\right)^k \quad (\text{B12})$$

$$= 1 + \frac{\beta(c-R)(1-2q)}{1+2R} \left[1 - \left(1 - \frac{1+2R}{N}\right)^k\right]. \quad (\text{B13})$$

Since  $\Delta p_k$  goes to zero as  $k$  goes to infinity, the steady-state distribution  $p_s$  is obtained by taking  $k \rightarrow \infty$  limit of Eq. (B13). It is given by

$$p_s(q, k\Delta t) = \lim_{k \rightarrow \infty} p(q, k\Delta t) \quad (\text{B14})$$

$$= 1 + \frac{\beta(c-R)(1-2q)}{1+2R}. \quad (\text{B15})$$

Now we get the mean cooperation  $Q_s^{\text{MF}}$  in the steady state by

$$Q_s^{\text{MF}} = \int_0^1 q \left[1 + \frac{\beta(c-R)(1-2q)}{1+2R}\right] dq \quad (\text{B16})$$

$$= \frac{1}{2} + \frac{\beta(R-c)}{6+12R} \quad (\text{B17})$$

and see that  $R_b^{\text{MF}}$  in the weak selection limit is given by

$$R_b^{\text{MF}} = c \quad (\text{B18})$$

since  $Q_s^{\text{MF}} - 1/2$  is positive, zero, and negative for  $R > c$ ,  $R = c$ , and  $R < c$ , respectively.

### APPENDIX C: SYSTEM SIZE DEPENDENCE OF $R_b$ FOR $\beta = \infty$

We find  $R_b$  for  $c = 0.8$  and  $c = 0.9$  in the strong selection limit ( $\beta = \infty$ ) for five different population sizes of  $N = 50, 100, 200, 400,$  and  $800$  each. They are plotted against  $1/N$  in Figs. 7(a) and 7(b). The boundary values  $R_b$  decreases with increasing population sizes. The finite-size effect does not seem to follow a  $1/N$  correction. In Figs. 7(c) and 7(d), we adjust the exponent  $\gamma$  so that data lie on straight lines when they are plotted against  $1/N^\gamma$ . The lines in Figs. 7(c) and 7(d) are given by  $R_b = R_b^\infty + AN^{-\gamma}$  with  $\gamma = 0.65, A = 2.35$  and  $R_b = 0.38$  for Fig. 7(c) and with  $\gamma = 0.65, A = 1.35$  and  $R_b = 0.78$  for Fig. 7(d). If this trend continues to infinite  $N$ , we get the boundary value of the infinite population  $R_b^\infty = 0.38$  for  $c = 0.8$  and  $0.78$  for  $c = 0.9$ .

### APPENDIX D: CHAIN-REACTION DEATH ON A SCALE-FREE NETWORK

We study the chain-reaction death model on scale-free (SF) networks which are generated by Barabási-Albert (BA) algorithm [25]. We grow the network from an initial seed of two (connected) nodes by attaching new nodes one by one. When we add a node, we select two nodes in the network proportionally to their current degrees and connect the new node to the selected nodes. The network grows until its size becomes  $N = 200$ .

Unlike the cycles considered in the main text, nodes on the SF networks have different numbers of neighbors. Due to this heterogeneity in degrees, individuals in the SF network play a different number of games. Now we need to consider the cost  $g$  to play a game in addition to the cost  $c$  of cooperation. The

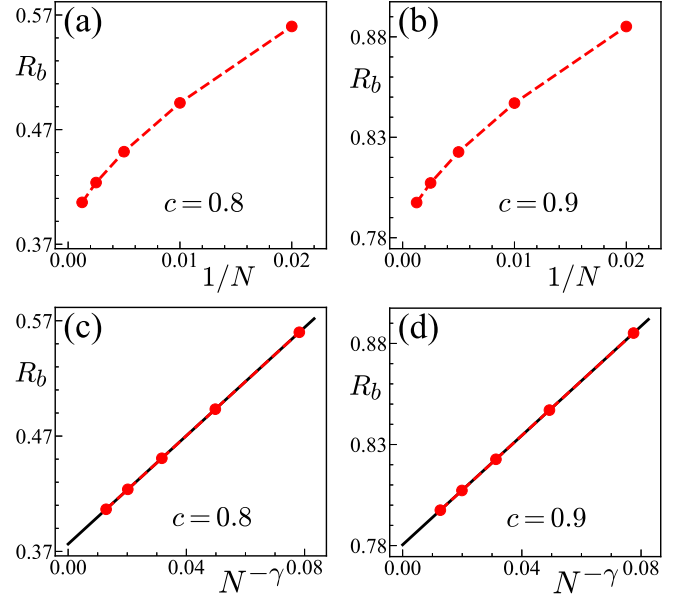


FIG. 7. System size dependence of  $R_b$  for  $c = 0.8$  and  $c = 0.9$  in the strong selection limit of  $\beta = \infty$ . The boundary values  $R_b$  are measured for  $N = 50, 100, 200, 400,$  and  $800$  and plotted against  $1/N$  for (a)  $c = 0.8$  and (b)  $c = 0.9$ . In (c) and (d), they are plotted against  $1/N^\gamma$  with  $\gamma = 0.65$  for both (c) and (d). The lines in (c) and (d) are given by  $R_b = R_b^\infty + AN^{-\gamma}$  with  $\gamma = 0.65, A = 2.35,$  and  $R_b = 0.38$  for (c) and with  $\gamma = 0.65, A = 1.35,$  and  $R_b = 0.78$  for (d).

payoff matrix becomes

$$\begin{array}{c} C \\ D \end{array} \begin{array}{cc} C & D \\ \left( \begin{array}{cc} 1-c-g & -c-g \\ 1-g & -g \end{array} \right), \end{array} \quad (\text{D1})$$

where we normalize the benefit of cooperation  $b$  as a unit value as in the main text. The total payoff  $\pi_i$  of member  $i$  is now given by

$$\pi_i = -k_i(cq_i + g) + \sum_{j \in S_i} q_j \quad (\text{D2})$$

$$= \pi_i^0 - gk_i, \quad (\text{D3})$$

where  $k_i$  is the degree of member  $i$ ,  $S_i$  is the set of neighbors of member  $i$ , and  $\pi_i^0$  is the payoff without the game cost  $g$ . For cycles, all members have the same degree  $k_i = 2$ , and the game cost  $g$  does not affect strategy evolution since the death probability of member  $i$

$$p_i^d = \frac{1}{Z} e^{-\beta\pi_i} = \frac{1}{e^{2\beta g} Z_0} e^{-\beta\pi_i^0 + 2\beta g} \quad (\text{D4})$$

$$= \frac{1}{Z_0} e^{-\beta\pi_i^0} \quad (\text{D5})$$

is independent of  $g$ . Here  $Z_0 = \sum_i e^{-\beta\pi_i^0}$ . However, for SF networks, the death probability  $p_i^d \propto e^{-\beta\pi_i} = e^{\beta g k_i} e^{-\beta\pi_i^0}$  strongly depends on  $g$  especially for hubs whose degree  $k_i$  is large.

We investigate the evolution dynamics with two different values of the game cost,  $g = 0$  and  $g = \frac{1-c}{2}$ . The latter is



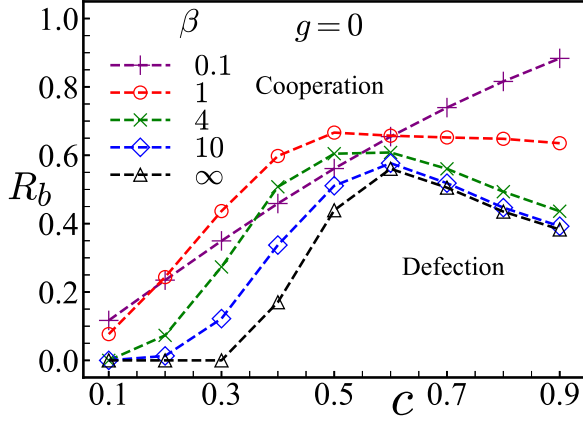


FIG. 8. The phase boundaries between cooperative and defective regions in the  $R$ - $c$  parameter space for  $g = 0$ .  $R_b$  values for  $\beta = 0.1$  (pluses), 1 (circles), 4 (crosses), 10 (diamonds), and  $\infty$  (triangles) are represented at  $c = 0.1, 0.2, \dots, 0.9$ .

chosen such that the average payoff per game is zero when players decide their actions randomly. In other words, the death probability  $p_i^d$  of member  $i$  becomes independent of its degree  $k_i$  when all members choose their actions at random.

For a given set of parameters  $c, g, R$ , we perform  $M = 1000$  independent simulations and measure the average cooperation probability of the population in the steady states. Each simulation is performed on a different SF network which is grown independently with the BA algorithm.

Figure 8 shows the phase boundaries between cooperative and defective regions in the  $R$ - $c$  parameter space for  $g = 0$ . For given  $c$  and  $\beta$  (with  $g = 0$ ), we measure the mean cooperation  $Q_s$  in steady states for a series of  $R$  values and find  $R_b$  such that  $Q_s(R = R_b) = 0.5$ .  $R_b$  values for  $\beta = 0.1, 1, 4, 10$  and  $\infty$  are denoted by plus, circle, cross, diamond, and triangle symbols, respectively, at  $c = 0.1, 0.2, \dots, 0.9$  in Fig. 8.

There are two notable features in this figure. First, the cooperative region is smaller comparing to Fig. 6 for the cycle population in the main text. At first glance, this looks like a puzzle. A selfish player on a hub is more likely to be eliminated through a CRD than a selfish player on a peripheral site because the former has more potential FDD sites in its neighbors. Since the influence of hubs is more significant than that of peripheral sites in general, we naturally expect CRD processes may promote cooperation more efficiently on SF networks. However, Fig. 8 shows that the cooperative regions are smaller on SF networks than on cycles. For example, when  $\beta = \infty$  and  $c = 0.5$ , the SF population evolves to cooperation only for  $R \gtrsim 0.45$  while the cycle population does for almost any positive  $R$ .

To understand this unexpected feature, we analyze the payoff distribution at hub sites. For  $g = 0$ , the payoff of member  $i$  can be written as

$$\pi_i = k_i(Q_i - cq_i), \quad (\text{D6})$$

where  $Q_i = \frac{1}{k_i} \sum_{j \in S_i} q_j$  is the average cooperation probability of the neighbors of member  $i$ . When  $q_i$  is smaller than  $Q_i/c$ ,  $Q_i - cq_i$  is positive and  $\pi_i$  becomes very large for  $k_i \gg 1$ . Hence the player at a hub site (say, site  $i$ ) is unlikely to die by FDD if  $q_i < Q_i/c$ . On the other hand, if the hub is cooperative,

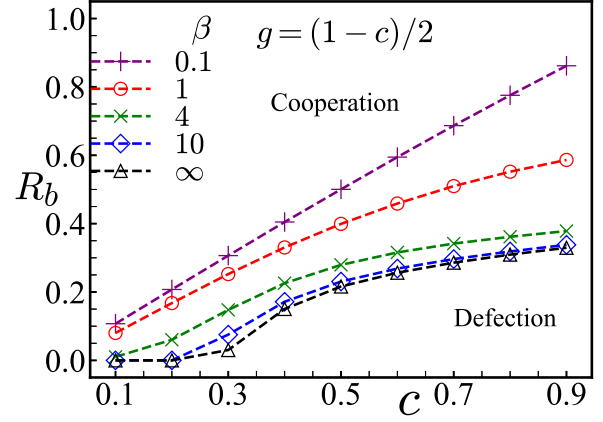


FIG. 9. The boundaries between cooperative and defective phases in the  $R$ - $c$  parameter space are presented for  $\beta = 0.1$  (pluses), 1 (circles), 4 (crosses), 10 (diamonds), and  $\infty$  (triangles).  $R_b$  values are obtained at  $c = 0.1, 0.2, \dots, 0.9$  for each  $\beta$  and  $N = 200$  for all cases.

than it can avoid CRD by providing enough payoff to its neighbors. Therefore, unless  $c$  is close to 1, a cooperative hub with selfish defective neighbors becomes stable when

$$Q_i < q_i < Q_i/c. \quad (\text{D7})$$

For  $c = 1/2$ , the above inequality becomes

$$Q_i < q_i < 2Q_i, \quad (\text{D8})$$

which holds, for example, when  $q_i = 0.6$  and  $Q_i = 0.4$ . In this case, the population lies in a defective phase since the number of hubs is much smaller than the number of their neighbors.

This observation also explains the other feature of our model on SF network (with  $g = 0$ ). According to Fig. 8, the defective regions in the  $R$ - $c$  parameter space decrease as  $c$  increases for  $c \gtrsim 0.6$  and  $\beta \gtrsim 1$ . Recall that the cost  $c$  is the “equal gain” of switching from C to D, i.e., the level of the temptation for defection. Hence it is natural to expect the defective region to increase as  $c$  increases. However, for  $c \gtrsim 0.6$ , Fig. 8 shows the opposite when  $\beta$  is large. Note that the larger the  $c$  value, the smaller the range of  $q_i$  that satisfies inequality (D7). Therefore, the defective community consists of an altruistic hub surrounded by selfish neighbors becomes unstable, and the defective phase regions decrease as the cost  $c$  increases for large  $c$ .

We now consider the case of  $g = \frac{1-c}{2}$  in which the payoff matrix of Eq. (D1) becomes

$$\begin{array}{cc} & \begin{array}{c} C \\ D \end{array} \\ \begin{array}{c} C \\ D \end{array} & \begin{pmatrix} \frac{1-c}{2} & \frac{-1-c}{2} \\ \frac{1+c}{2} & \frac{-1+c}{2} \end{pmatrix}. \end{array} \quad (\text{D9})$$

The sum of all elements in the matrix is zero. Therefore, when all members choose their actions randomly, the average payoff is zero, and the probability to be an FDD site becomes independent of the degree of the site. As in the case of  $g = 0$ , we perform MC simulations for a series of  $c$  and  $R$  values and measure the population average of the cooperation probabilities to obtain the phase boundary between cooperative

and defective regions. Figure 9 shows the phase diagram. The plus, circle, cross, diamond, and triangle symbols denote the  $R_b$  values for  $\beta = 0.1, 1, 4, 10$ , and  $\infty$ , respectively.

Note that the unusual negative slopes of  $R_b(c)$  (observed in Fig. 8) disappear in Fig. 9, and the defective region monotonically grows as the cost  $c$  increases. For  $c = 1$ , the game cost  $g = (1 - c)/2 = 0$  and hence the  $R_b$  values are the same as in Fig. 8. As  $c$  decreases from 1,  $g$  increases and the cost for the

games  $k_i g$  for the hubs becomes large. This makes it hard for the hub to be an altruist unless it receives enough cooperation from its neighbors. An altruistic hub with selfish neighbors is prone to be an FDD site since it pays costs for its cooperative actions in addition to game costs. This makes the exploitation of altruistic hub become unstable. Therefore, assortments between cooperators are enhanced, and the cooperative region increases as  $c$  decreases.

- 
- [1] M. A. Nowak, *Science* **314**, 1560 (2006).
- [2] M. A. Nowak, C. E. Tarnita, and E. O. Wilson, *Nature (London)* **466**, 1057 (2010).
- [3] P. Abbot, J. Abe, J. Alcock, S. Alizon, J. A. Alpedrinha, M. Andersson, J.-B. Andre, M. Van Baalen, F. Balloux, S. Balshine *et al.*, *Nature (London)* **471**, E1 (2011).
- [4] J. A. R. Marshall, *Trends Ecol. Evol.* **26**, 325 (2011).
- [5] S. K. Baek, H.-C. Jeong, C. Hilbe, and M. A. Nowak, *Sci. Rep.* **6**, 25676 (2016).
- [6] G. Szabó and G. Fath, *Phys. Rep.* **446**, 97 (2007).
- [7] M. Perc and A. Szolnoki, *Biosystems* **99**, 109 (2010).
- [8] H.-C. Jeong, S.-Y. Oh, B. Allen, and M. A. Nowak, *J. Theor. Biol.* **356**, 98 (2014).
- [9] J. A. Fletcher and M. Doebeli, *Proc. R. Soc. Lond. B* **276**, 13 (2009).
- [10] F. Débarre, C. Hauert, and M. Doebeli, *Nat. Commun.* **5**, 3409 (2014).
- [11] S. Park and H.-C. Jeong, *J. Korean Phys. Soc.* **60**, 311 (2012).
- [12] H. Ohtsuki, C. Hauert, E. Lieberman, and M. A. Nowak, *Nature (London)* **441**, 502 (2006).
- [13] H. Ohtsuki and M. A. Nowak, *J. Theor. Biol.* **243**, 86 (2006).
- [14] C. E. Tarnita, T. Antal, H. Ohtsuki, and M. A. Nowak, *Proc. Natl. Acad. Sci. USA* **106**, 8601 (2009).
- [15] Z. Wang, S. Kokubo, J. Tanimoto, E. Fukuda, and K. Shigaki, *Phys. Rev. E* **88**, 042145 (2013).
- [16] J. Maynard Smith, *Evolution and the Theory of Games* (Cambridge University Press, Cambridge, 1982)
- [17] The CRD process represents the dynamical effects of the “sudden” disappearance of a neighbor. The sudden disappearance and the absence from the beginning may result in different consequences. For example, consider the case where firm A contracts to supply 100 products to firm B assuming that firms C and D provide 50 parts each to firm A. If firm D bankrupts and fails to supply 50 parts, firm A may not be able to keep the contract with firm B. This is different from the case when firm A contracts to supply 50 products to firm B assuming that only firm C provides 50 parts.
- [18] P. Bak and K. Sneppen, *Phys. Rev. Lett.* **71**, 4083 (1993).
- [19] M. A. Nowak, *Evolutionary Dynamics* (Harvard University Press, Cambridge, MA, 2006).
- [20] B. Allen, G. Lippner, Y.-T. Chen, B. Fotouhi, N. Momeni, S.-T. Yau, and M. A. Nowak, *Nature (London)* **544**, 227 (2017).
- [21] H. Ohtsuki and M. A. Nowak, *Proc. R. Soc. Lond. B* **273**, 2249 (2006).
- [22] J. Bahk, S. K. Baek, and H.-C. Jeong, *Phys. Rev. E* **99**, 012410 (2019).
- [23] H. Flyvbjerg, K. Sneppen, and P. Bak, *Phys. Rev. Lett.* **71**, 4087 (1993).
- [24] P. Bak, *How Nature Works: The Science of Self-organized Criticality* (Springer Science & Business Media, New York, 2013).
- [25] A.-L. Barabási and R. Albert, *Science* **286**, 509 (1999).